ACADÉMIE
DES SCIENCES
INSTITUT DE FRANCE

Comptes Rendus
Physique

Pawel Pieranski and Maria Helena Godinho

The Toulouse–Kleman homotopic classification of topological defects in ordered systems illustrated by experiments

Volume 25 (2024), p. 367-388

Online since: 11 December 2024

https://doi.org/10.5802/crphys.206

The Comptes Rendus. Physique *are a member of the Mersenne Center for open scientific publishing*
www.centre-mersenne.org — e-ISSN : 1878-1535

ACADÉMIE DES SCIENCES
INSTITUT DE FRANCE

Comptes Rendus. Physique
2024, Vol. 25, p. 367-388
https://doi.org/10.5802/crphys.206

Research article / *Article de recherche*

The Toulouse–Kleman homotopic classification of topological defects in ordered systems illustrated by experiments

Classification Toulouse–Kleman de défauts topologiques dans les systèmes ordonnés, illustrée par des expériences

Pawel Pieranski [a, *] **and Maria Helena Godinho** [b]

[a] Laboratoire de Physique des Solides, Université Paris-Saclay, Orsay, France

[b] i3N/CENIMAT, Department of Materials Science, NOVA School of Science and Technology, NOVA University Lisbon, Campus de Caparica, Caparica 2829 - 516, Portugal

E-mails: pawel.pieranski@universite-paris-saclay.fr (P. Pieranski), mhg@fct.unl.pt (M. H. Godinho)

Abstract. Classification of defects in ordered systems, based on the homotopy theory, conceived by Gérard Toulouse and Maurice Kléman has a very wide range of applications. We illustrate its *modus operandi* with three experimental examples. We deal first with dislocations in a dissipative periodic pattern of convection rolls in a shear flow instability in nematics. As the second example we chose the captive disclination loops threaded on polymer fibers immersed in nematics. Third, we focus on objects with double topological character defined for the first time in the generic article coauthored by Gérard Toulouse: the "double et tripple anneau" Hopf links made of interlaced dislocation loops in cholesterics. Finally, we report on the recent discovery of their generalised, beads necklace version made of many minimal dislocation loops threaded, like pearls, on a string-like dislocation loops.

Résumé. La classification de défauts dans les systèmes ordonnés, basée sur la théorie de homotopie, conçue par Gérard Toulouse et Maurice Kleman a des nombreuses applications. Nous illustrons son *modus operandi* avec trois exemples expérimentaux. D'abord, nous considérons les dislocations dans un système dissipatif périodique fait de rouleaux de convection d'une instabilité de cisaillement d'un nématique. Le deuxième example est celui de disinclinaisons captives enfilées sur une fibre polymérique immergée dans un nématique. En troisième lieu, nous nous intéressons aux objets à caractère topologique double définis pour la première fois dans un article générique cosigné par Gérard Toulouse : les liens de Hopf faits de deux et trois dislocations annulaires dans un cholestérique. Finalement, nous annonçons la découverte de la version généralisée - colliers faits d'une multitude d'anneaux minimaux enfilés sur une dislocations porteuse.

Keywords. topological defects, dislocations, knots, links, tangles.

Mots-clés. défauts topologiques, dislocations, noeuds, liens, torsades, cholestériques.

Electronic supplementary material. Videos 1 to 11 are available as supplementary material from the journal's website under the article's URL or from the author.

Manuscript received 6 May 2024, revised 27 August 2024, accepted 5 September 2024.

* Corresponding author

1. Classification of topological defects in ordered media

1.1. *The birth of a new concept*

The article untitled "Principles of a classification of defects in ordered media" cosigned by Gérard Toulouse and Maurice Kleman [1] is a temporal mile-stone marking the birth of the unifying concept of "topological defects" that crowned the stay of Gérard Toulouse at the Laboratoire de Physique des Solides (LPS) in Orsay.

This birth was the result of fertile interactions between Toulouse and Kleman in a laboratory renown among others to studies of defects in condensed matter systems such as dislocations in solid crystals (Jacques Friedel [2, 3]), vortices in superconductors and superfluids (Pierre-Gilles de Gennes [4, 5]) or domain walls and singular points in magnets (Maurice Kleman). This diversity of defects in systems equipped with different order parameters increased considerably since 1969 when several young teams started to work on liquid crystals (headed by G. Durand, E. Guyon, M. Kleman, M. Veyssie). The liquid crystalline states of matter being liquid in three (nematics, cholesterics), two (smectics), or one (columnar) dimensions, are fragile and therefore frequently full of defects, such as disclinations and dislocations. These defects are extremely easy to generate by phase transitions, flows or elastic strains. One could even say that the issue is not "how to generate them" but "how to get rid of them". Moreover they are easy to observe in an optical microscope.

Maurice Kleman, who worked previously on domain walls in magnets, started in 1969 to investigate intensively defects in liquid crystals with his students and visitors as well as in collaboration with other members of LPS and in particular with Gérard Toulouse.

In this favourable ambience, Toulouse and Kleman, who both had predilection for the mathematical abstraction, succumbed, fortunately, to it and embraced in one single glance the whole wide panorama of topological defects in condensed matter [1].

As a PhD student, one of the autors (P.P.) had the chance to listen to the wonderful lectures of Toulouse on topology in mathematics and physics illustrated by beautiful drawings made simultaneously with chalk on a black-board. Today we know that we had the privilege to hear Toulouse speaking about a new concept *in statu nascendi*. His explanations of classification of topological defects in condensed matter based on homotopy theory were crystal-clear.

1.2. *Contents of this paper*

Our aim here will be not to discuss the Toulouse–Kleman theory from the formal point of view because today it is widely known and explained in an accessible manner, for example, in the book of Kleman and Lavrentovich [6] or in the excellent review papers of Kurik and Lavrentovich [7] and of Smalyukh [8]). Instead of that we will illustrate its *modus operandi* using as typical examples three experiments realised in the Laboratoire de Physique des Solides in Orsay.

Before that, it is important to stress that the theory of Toulouse and Kleman is applicable not only to topological defects in crystals or liquid crystals but also to vortices in classical fluids and superfluids [9], superconductors [10], electromagnetic waves [11] as well as to defects in periodic dissipative patterns [12, 13] such as:

(1) Rayleigh–Benard instabilities [14],
(2) shear flow instabilities in nematics [15],
(3) Faraday instability [16],
(4) Taylor instability [17].

For this last reason, as the first example we discuss in Section 2 point defects in two-dimensional patterns of the *shear flow instability in nematics* [15] that was discovered, under

the supervision of Etienne Guyon [18], during the stay of Gérard Toulouse in the Laboratoire de Physique des Solides in Orsay.

The second example discussed in Section 3 is that of the so-called *captive disclination loops in nematics* [19]. It concerns a peculiar texture, made of disclination loops threaded on a polymer fiber, which has the *double topological character* defined for the first time in the generic collective paper coauthored by Gérard Toulouse [20]. Indeed, on one hand, disclinations in nematics are linear topological defects of the nematic order parameter. On the other hand, the presence of the polymeric fiber alters the topology of the three-dimensional space and by this means prevents the collapse of the disclination loop.

For the sake of clarity, before the discussion in Sections 5 and 6 of the Hopf links and of necklaces made of dislocations, we need to introduce first in Section 4 the concept of dislocations in cholesterics which is subtle enough on its own.

The last experimental illustration of the Toulouse–Kleman theory discussed in Sections 5 and 6 concerns also textures with the *double topological character* made, in this case, of linked dislocation loops in cholesterics. We point out that recent experiments confirmed the finding and conjectures of the reference [20]. Let us stress that the most recent experiment on the genesis of *necklaces made of dislocation loops* was realised during corrections of the original manuscript.

The concept of distortions with double topological character extends to knots made of dislocation in cholesterics. They are discussed extensively in another article inspired by works of Gérard Toulouse and Maurice Kleman [21].

2. Dislocation in the flow pattern of a shear flow instability in nematics

The shear flow instabilities in nematics occur in a nematic layer confined between two parallel glass plates providing the so-called homeotropic (orthogonal to glass surfaces, parallel to the z axis) anchoring of molecules. In the absence of flows, orientations of molecules in the bulk of the nematic layer described by the director field $\vec{n}$ are the same: $\vec{n}(x,y,z) = (0,0,1)$ (vertical red lines in Figure 1 (c)).

The upper and lower plates are then submitted to sinusoidal oscillations in respectively x and y directions: $X_o \sin(\omega t)$ and $Y_o \cos(\omega t)$. By this means an elliptic shear flow is driven inside the nematic layer (see Figure 1 (a)).

When the product $X_o Y_o$ of the oscillations' amplitudes crosses a threshold value, the stationary convection pattern shown in Figure 1 (b) appears. It is made of rolls parallel to the η axis depicted schematically in Figure 1 (a). The flow profile in the centre of one roll is approximately sinusoidal $v_\xi = v_o sin(2\pi z/h)$ (see Figure 1 (d)). The velocity gradient $s = \partial v_\xi \partial z$ alters the initially homogenous vertical orientation of the molecules. One can infer from the optical contrast between crossed polarizers that tilt angle θ defined in Figure 1 (d) varies periodically in the ξ direction orthogonal to the rolls:

$$\theta \approx \theta_o \sin(q\xi + \varphi) \tag{1}$$

where $q = 2\pi/\lambda$ is the wave vector and φ is the phase.

This tilt angle plays the role of the order parameter resulting from the symmetry breaking. Its amplitude θ_o grows from zero in the ground state to some finite value during the unset of the instability after the crossing of the critical value of the excitation parameter $X_o Y_o$.

The phase φ sets the position of the roll pattern on the ξ axis. When the whole pattern is shifted by $\delta\xi$ in the ξ direction, the phase varies by $\delta\varphi = 2\pi\delta\xi/\lambda$.

Using the vocabulary of the Toulouse–Kleman theory, we can say that the degeneracy space of the order parameter θ is topologically equivalent to a circle along which the phase φ varies between 0 and 2π (see Figure 1 (c)).

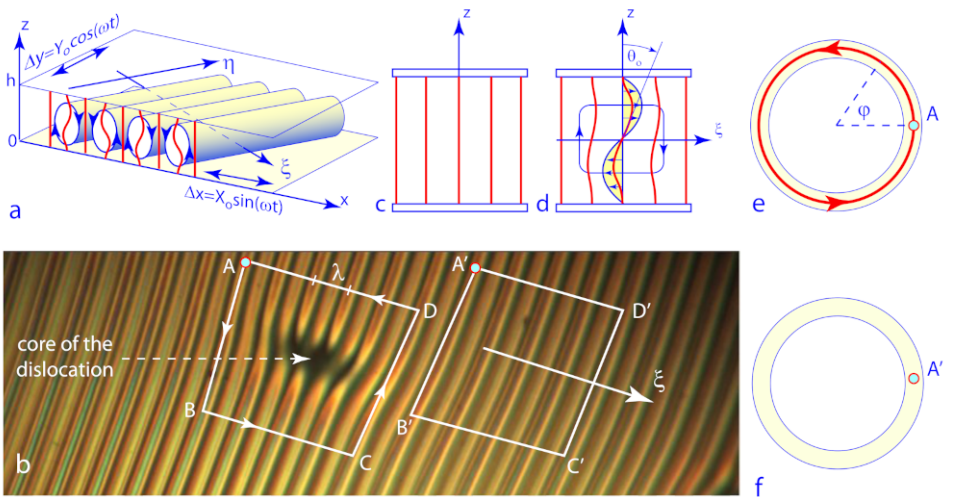

Figure 1. Application of the Toulouse–Kleman theory to the case of the periodic pattern of a shear flow instability in nematics. a) Perspective view of the experiment. b) View of the instability observed between crossed polarizers. c) Initial homogeneous orientation $\vec{n} = (0,0,1)$ of the director field parallel to the nematic molecules. d) Deformation of the director field induced by the velocity gradients inside the convection rolls. e-f) Degeneracy space of the periodic order parameter θ. e) Mapping of the trajectory along the quadrilateral ABCDA in real space onto the degeneracy space of the order parameter. The integral $\oint_{ABCDA} \delta\varphi = 2\pi$ unveils the presence of the dislocation inside the quadrilateral ABCDA. f) In the absence of the dislocation one has: $\oint_{A'B'C'D'A'} \delta\varphi = 0$. (see video 1)

For readers familiar with the concept of dislocations in crystals it is obvious that the pattern in Figure 1 (b) contains a defect - a dislocation. Inside the core of the dislocation the amplitude of the order parameter θ_o tends to zero. For this reason it appears as the small black area when observed between crossed polarizers.

In terms of the Toulouse–Kleman theory, the dislocation in the pattern of the convection rolls is characterised by the value 2π of the integral calculated along the closed circuit ABCDA surrounding the black core:

$$\oint_{ABCDA} \delta\varphi = 2\pi \tag{2}$$

Let us emphasize that this value 2π does not depend on the size of the integration circuit as long as the black area – the core of the dislocation – is located inside it. On the other hand, the value of the same integral calculated along the circuit A'B'C'D'A' is zero which means that there is no dislocation inside it.

$$\oint_{A'B'C'D'A'} \delta\varphi = 0 \tag{3}$$

3. Captive π disclinations in nematics

3.1. *Experiment*

The first experiment deals with the so-called "captive disclination loops" [19]. Its principle is represented schematically in Figure 2 (a) where a disclination loop, the red circle, is tethered on a polymer fiber immersed in a nematic liquid crystal contained between two parallel glass slides.

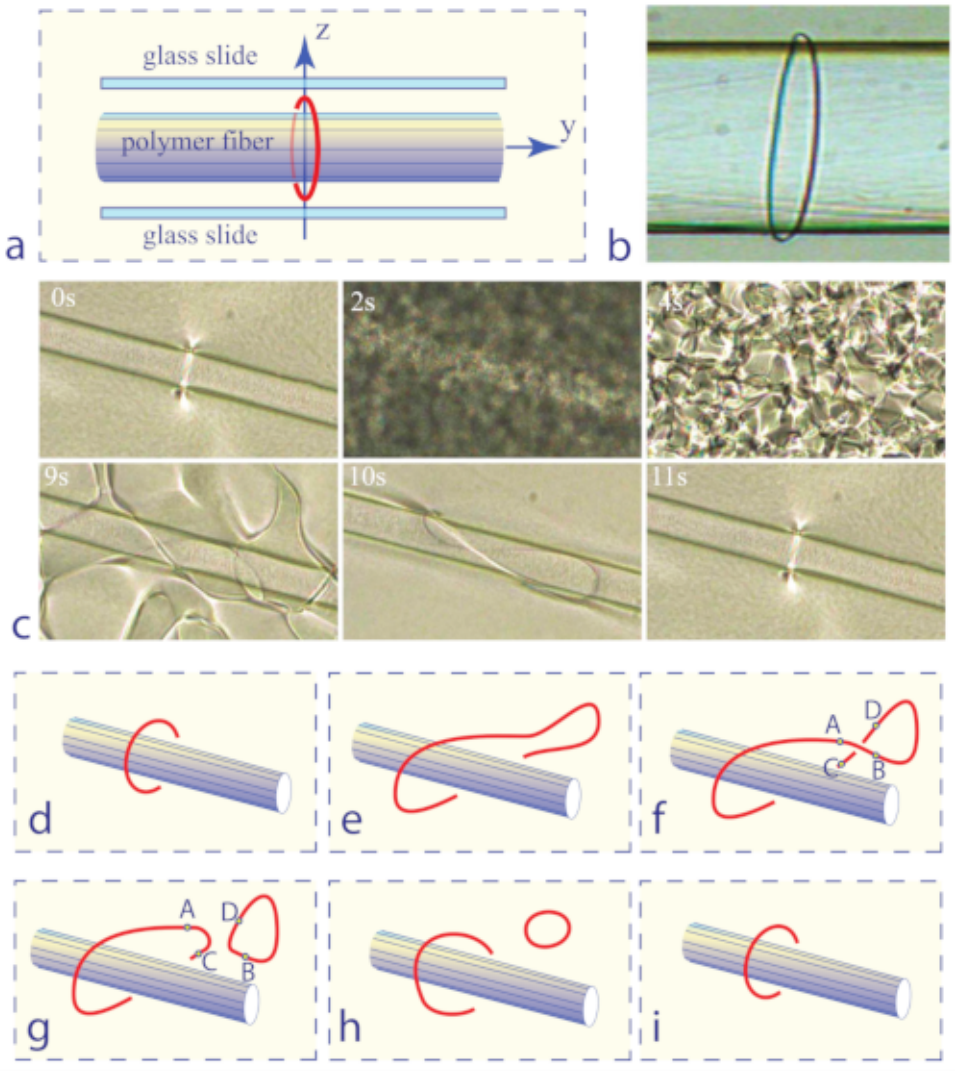

Figure 2. Experiment with a disclination loop tethered on a fiber. a) Geometry of the experiment. b) View of the tethered loop at equilibrium. c) Stretching of the captive loop by a turbulent flow and relaxation to the equilibrium. d-e) Stretched captive loop. f-g) Splitting of the stretched loop by rewiring of the self-crossing $AB + CD \Rightarrow AC + BD$. h-i) Relaxation: the tethered loop recovers its initial shape, the free loop collapses. (see video 2)

Surfaces of the slides, coated with lecithin, orient the molecules of the nematic in the direction z perpendicular to them (homeotropic anchoring). The surface of the polymer fiber (a nylon fishing line) orients the nematic molecules in the direction y parallel to it (planar anchoring).

This disclination loop observed with a microscope (in transmitted light) from the z direction appears as a black line in Figure 2 (b). As we will see in the next section, it corresponds to a linear singularity of the molecular orientations which are usually represented by a unitary field **n**, called director, locally parallel to the molecules. This linear singularity of the director field results in a singularity of the refractive index. Therefore, the disclination refracts the light so much that it appears in transmitted light as the black line.

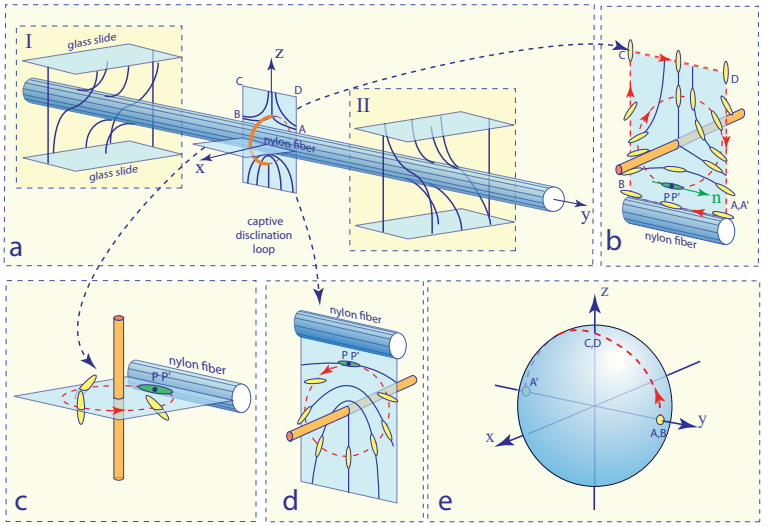

Figure 3. Analysis of the tethered disclination loop in terms of the homotopy theory. a) Perspective view of the director field. b-d) Director field in the vicinity of the disclination. e) Mapping of the director field from the closed trajectories in real space onto the unit sphere. (see video 3)

The series of six pictures in Figure 2(c) shows that this captive disclination loop cannot removed from the fiber by breaking it. This does not mean that it is very strong. On the contrary, it is topologically resilient. Indeed, the second picture labelled "2s" shows that the turbulent flow, due to an electrohydrodynamic instability, stretches and deforms this tethered disclination loop so much that it "falls into pieces" by the rewiring processes similar to the one depicted in pictures d to g. For this reason in the picture labeled "2s" the sample appears as turbid (almost black) – the illuminating light beam is almost completely diffused by the swarm of new disclination loops. The next four pictures show that once the turbulent flow is switched off, the tethered disclination recovers in a few seconds its initial length, shape and position due to the orientational elasticity of nematics, and which is the most important: it remains tethered on the polymer fiber. All other loops that were generated by the rewiring processes are free so that they collapse like the one in pictures g-i.

3.2. *Interpretation in terms of the homotopy theory*

Let us interpret now results of this simple experiment in terms of the theory proposed by Toulouse and Kleman. To start with, let us remind that the nematic mesophase is characterised by an orientational order parameter. In nematics, contrary to the isotropic phase, orientations of molecules are not random. In the ground state, molecules are in average parallel to one direction indicated by the unit vector **n** called director.

In the absence of fields and surfaces, the director can take any direction. The set of all possible directions that can be taken by the director can be represented by the unit sphere drawn in Figure 3(e). In this case we would say the degeneracy space R_N of nematics is a two-dimensional sphere S^2. However, in non polar nematics, directions **n** and $-\mathbf{n}$ are equivalent so that degeneracy space R_N of the director in not the sphere S^2 but the sphere S^2 factored by the group Z_2: $R_N = S^2/Z_2$. In other words, the states corresponding to antipodal pairs of points on the unit sphere are the same.

In the experiment described above, the director field $\mathbf{n}(x,y,z)$ cannot be uniform because it must match the limit (anchoring) conditions: $\mathbf{n}//z$ on glass slides and $\mathbf{n}//y$ on the fiber surface.

As required, fields $\mathbf{n}_I$ and $\mathbf{n}_{II}$, represented by black lines in the two regions labeled as "I" and "II" in Figure 3 (a), located respectively on the left and hand sides of the disclination loop, match these anchorings conditions. Let us stress that these drawings are not results of calculations; they were made by hand. Nevertheless, they are sufficient from topological point of view.

Let us remark now that these two fields are not identical: the field $\mathbf{n}_I$ is the reflection of the field $\mathbf{n}_{II}$ in the plane (x,z). The issue is now: "can such two symmetrical fields $\mathbf{n}_I$ and $\mathbf{n}_{II}$ be connected in a continuous manner?". The answer given by the homotopy theory is: "No", there must be a singular line – the disclination – on which the direction of molecules (of the director $\mathbf{n}$) is not well defined.

To get this answer, the homotopy theory proceeds as follows. Let us consider the rectangular closed trajectory ABCD with points A and D located on the nylon surface, while the points B and C are located on the glass slide. Segments AB and CD are located respectively on the left- and right-hand sides of the mirror plane (x,z).

Let us examine now how the director field varies along this trajectory. In the point A, the director is parallel to the y axis: $\mathbf{n}_A = (0,1,0)$. As the segment AB lies on the fiber surface, all along it the director field keeps its orientation so that at the point B we have $\mathbf{n}_B = (0,1,0)$. Let us mark this orientation $\mathbf{n}_{A,B} = (0,1,0)$ with a yellow small circle on the unity sphere drawn in Figure 3 (e). Along the segment BC, the director rotates around the x axis in the anticlockwise direction and varies from $\mathbf{n}_B = (0,1,0)$ to $\mathbf{n}_C = (0,0,1)$. Along the segment CD located on the slide surface, the director conserves its vertical orientation so that we have $\mathbf{n}_D = (0,0,1)$. This orientation $\mathbf{n}_{C,D} = (0,0,1)$ is labelled "CD" on the unit sphere in Figure 3 (e). Finally, along the last segment DA, the director rotates in anticlockwise direction around the axis x and arrives at A with orientation $\mathbf{n}_A = (0,-1,0)$. This final orientation of the director is marked with the second small circle on the unit sphere in Figure 3 (e).

In conclusion, variation of the director along the closed trajectory ABCD in real space is represented on the unit sphere by the trajectory connecting the two antipodal points marked with the yellow circles. In spite of the appearances, this trajectory is also closed because the directions $\mathbf{n}$ and $-\mathbf{n}$ are equivalent.

When the director field along the trajectory ABCD in real space surrounding the disclination is perturbed in a continuous manner, the corresponding trajectory on the unit sphere is perturbed too but it connects always two antipodal points. In general, the director field along all closed trajectories in real space surrounding the disclination line (such as the circular trajectory PP' in Figures 3 (b), (c) and (d)) is mapped on the unit sphere to trajectories connecting two antipodal points. As this property does not depend on the radius r of the circular trajectory, the director field must have a singularity in the limit $r \to 0$. This singularity is located at the captive disclination loop.

Remark 1. The captive disclination loop observed in experiments has thus a singular core. This type of disclination is called π because the director rotates by π on a circuit surrounding it.

Remark 2. If the fiber was replaced by a cylindrical volume of a nematic oriented in y direction, the disclination loop would collapse.

Remark 3. The disclination loop tethered on the polymer fiber cannot collapse because it is repelled by the fiber surface with the planar anchoring. One could say that it hovers at a constant altitude above the fiber surface.

4. Dislocations in cholesterics

In the next section of this memorial article devoted to Gérard Toulouse, we will focus on his another contribution to the field of topological defects in condensed matter published in the article untitled "Distortions with double topological character: the case of cholesterics" cosigned with Yves Bouligand, Valantin Poénaru, Bernard Derrida and Yves Pomeau.

This paper deals with the structure of Hopf links made of dislocations in cholesterics. Such objects have indeed a double topological character because, on one hand, dislocations are topological defects and, on the other hand, links (and knots) are archetypes of topological intricacies.

Our aim here is to present this pioneer work in light of recent experiments that allowed us to generate the Hopf links in cholesterics in a well controlled manner and to study in more details their features.

In 1978, the subject was initiated by interaction of Gérard Toulouse with Yves Bouligand, a biologist frequently visiting LPS in Orsay. Bouligand was interested initially by textures inside thin cuts of cuticles of insects and amphipods that he observed by means of an electronic microscope. After the outbreak of the interest in liquid crystals in France, Bouligand switched to observations, by means of a polarising microscope, of thin layers of cholesteric liquid crystals confined between glass plates. Like the chitin in cuticles, the molecules in cholesterics form in equilibrium helices of pitch p (Figure 4 (f)). In samples with a very large pitch, Bouligand observed for the first time pairs of interlaced dislocations loops – the Hopf links [22].

For the sake of clarity, before discussion of these nested topological oddities, we need to introduce first the concept of dislocations in cholesterics which is subtle enough on its own.

4.1. *Dislocations in Grandjean–Cano wedges*

The wedge-shaped cholesteric layers (plane/plane in Figure 4 (a) or cylinder/cylinder in Figure 4 (b)) observed in the microscope (see Figures 4 (c) and (d)) resemble topographic maps with patterns of contour lines which, in the case of cholesterics, indicate the variable number N of cholesteric pitches confined between the limit surfaces.

In the picture of Figure 4 (c), obtained with the plane/plane wedge geometry, we note the presence of two types of lines: *thin* and *thick* ones. The thin lines separate fields with N and $N+1/2$ of cholesteric pitches while the thick lines are frontiers between fields with N and $N+1$ pitches. In terms of the classification of topological defects, these two types of lines correspond to the two possible types of edge dislocations (see Figure 4 (e)) with Burgers vectors $b = p/2$ (thin lines) and $b = p$ (thick lines). For this reason, thick lines in Figure 4 (c) split into two thin lines.

4.2. *Singular director field of the thin $b = p/2$ dislocation, homotopy theory*

Since the pioneer work of Georges Friedel [25] it is well known that there is no sharp phase transition between the nematic and cholesteric mesophases; when the pitch p of the cholesteric mesophase tends to infinity, it becomes identical with the nematic phase.

For this reason, dislocations in cholesterics can be seen also as disclinations [26]. Indeed, along a closed circuit ABCDA surrounding a thin ($b = p/2$) dislocation, the director n rotates by π (see Figure 5 (c)). Therefore, using the same arguments as those concerning the captive disclination loops, the director field of the thin dislocation must be singular.

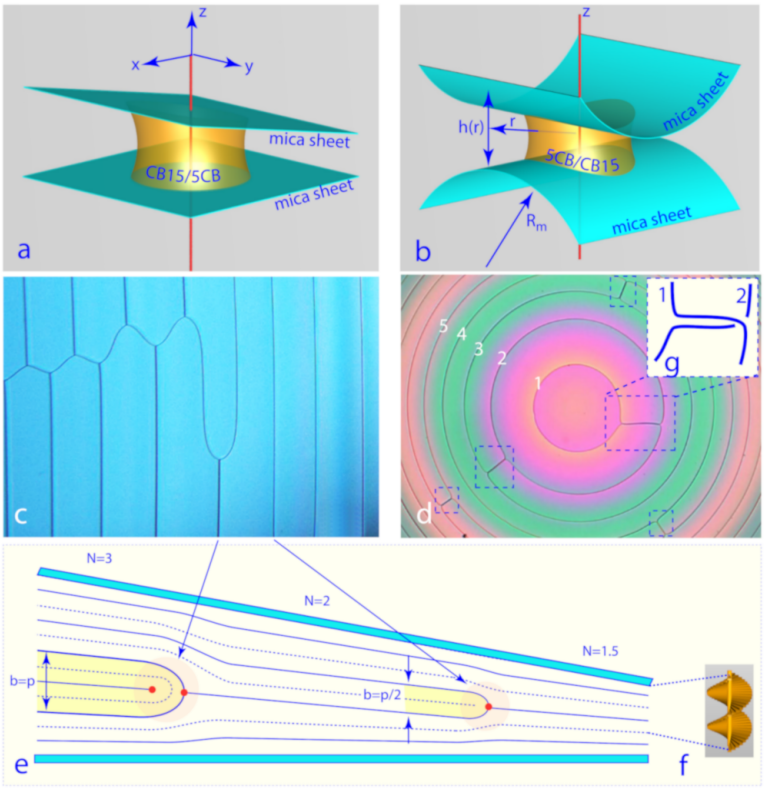

Figure 4. Dislocations in cholesterics confined between surfaces with planar anchoring. a) The plane/plane geometry of experiments of Bouligand [22]. b) The crossed cylinders geometry used in recent experiments [23, 24]. c) Dislocations' pattern in the plane/plane geometry. d) Dislocations' pattern in the cylinder/cylinder geometry. It corresponds to a multiply folded unknot. e) Cholesteric texture in the cross section of the dislocations' pattern in the plane/plane. f) Perspective view of the cholesteric helix. g) Two-level crossing of dislocations.

4.3. *Nonsingular director field of the thick b = p dislocation, homotopy theory*

The director field of the "thick" ($b = p$) dislocation in Figure 5 (a) seems also to be singular in points marked with red circles. However, examination of this director field in terms of the homotopy theory leads to a different conclusion.

Let us consider the evolution of the director along the closed circuit ABCDA surrounding the $b = p$ dislocation. Along the first segment AB, the director rotates by 2π around the z axis but along the rest of the circuit it does not rotate at all. As the overall rotation of the director along the circuit ABCDA is 2π, it is mapped onto the equator of the unit sphere (the degeneracy space of the director) where it is labelled "1" in Figure 5 (b).

In the same figure we show circles labeled from "1" to "5" which make the angle θ with the equator and are tangent to it in the point labelled "A". The radii of such oblique circles vary as $cos(\theta)$ and shrink from 1 (the equator) to 0 (point A). If φ is the curvilinear coordinate (azimuthal angle) that varies from 0 to 2π along each of the oblique circles, then the director field can be expressed as:

$$\mathbf{n}(\theta,\varphi) = \left[-\cos^2(\theta)\cos(\varphi) - \sin^2(\theta), -\cos(\theta)\sin(\varphi), \cos(\theta)\sin(\theta)(1-\cos(\varphi)\right] \tag{4}$$

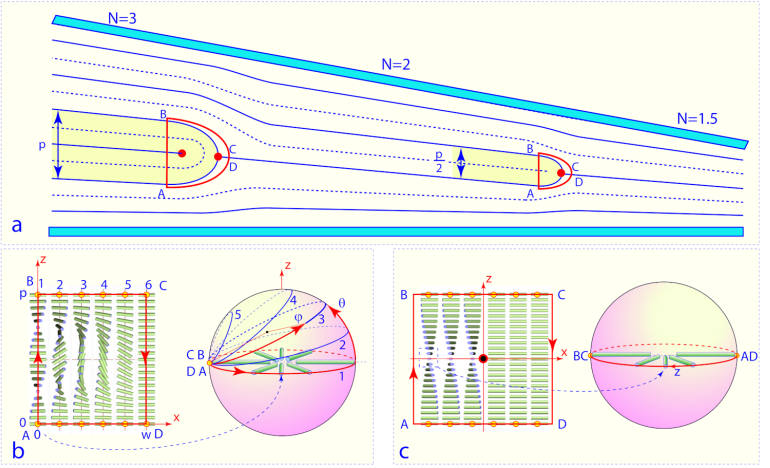

Figure 5. Dislocations in a cholesteric layer confined between two oblique planes. a) Definition of the *thick* and *thin* dislocations with Burgers vectors $b = p$ and $b = p/2$. b) Non singular director field of the thick dislocation. c) Singular director field of the thin dislocation.

Using the mapping rules $\varphi = 2\pi z/p$ and $\theta = (\pi/2)x/w$, the director can be transplanted from the unit sphere onto the rectangle $[0 < z < p,\ 0 < x < w]$ in real space. The resulting director field $\mathbf{n}(x,z)$ shown in Figure 5 (b) is nonsingular. In conclusion thanks to the homotopy theory we arrived at the conclusion that, in contradistinction with the thin $(b = p/2)$ dislocation, the director field of the thick $(b = p)$ dislocation is nonsingular.

4.4. *Kinks*

Figures 6 (a) and (b) show that the detailed texture of the director field of the thick $(b = p)$ dislocation depends on the mapping rules. The field in Figure 6 (b) was obtained using $\varphi = 2\pi(z - p/4)/p$ instead of $\varphi = 2\pi z/p$ used in Figure 6 (a).

In both textures the deformation of the director field $\vec{n}$ in the z direction $\partial\vec{n}/\partial z$ is the same. This means that the columns labeled $1, \ldots, 6$ in Figures 6 (a) and (b) are the same except for the rotation by $\pi/2$ around the z axis. However, the deformations of the director field $\vec{n}$ in the x direction $\partial\vec{n}/\partial x$ is different in the two textures. The texture in Figure 6 (b) involves the bend deformation while the one in Figure 6 (a) is rich in the splay deformation.

In 5CB (the nematic component of the chiral 5CB/CB15 cholesteric mixtures) the Frank constant K_{33} of the bend deformation is of the order of $7pN$ while the splay constant K_{11} is of the order of $5pN$. Knowing this, we can conclude that the total elastic energy of the director field in Figure 6 (b) is larger than that of the director field in Figure 6 (a).

For this reason, the tension T (energy per unit length) of the thick $(b = p)$ dislocation varies with its position z_D inside the cholesteric helix determined by the transplantation rule $\varphi = 2\pi(z - z_D)/p$. For $z_D = 0, p/2, p, 3p/2, \ldots$, T is minimal, while for $z_D = p/4, 3p/4, 5p/4, \ldots$ it is maximal. In the first approximation, we can write

$$T(z_D) \approx T_0 + \Delta T \sin^2(2\pi z_D/p) \tag{5}$$

with $\Delta T > 0$.

The thick $(b = p)$ dislocation parallel to the y axis has therefore the tendency to stay locked in one of the available energy minima of $T(z_D)$ occurring at $z_D = 0, p/2, p, 3p/2, \ldots$. Transitions

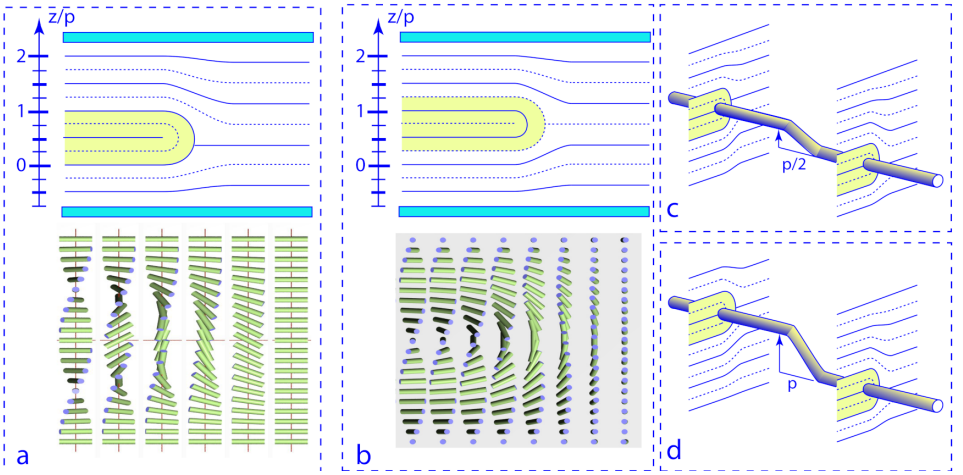

Figure 6. Kinks. a) Nonsingular director field of the thick ($b = p$) dislocation obtained through the transplantation rules $\varphi = 2\pi z/p$ and $\theta = (\pi/2)x/w$ (see Figure 5 (b)). b) Alternative director field obtained through the modified transplantation rule $\varphi = 2\pi(z - p/4)/p$. c) Kink of height p/2. d) Kink of height p.

between different minima are then mediated by localised kinks such as those depicted in Figures 6 (c) and 6 (d).

Experimental evidence for the existence of kinks is given below in Sections 6.5 and 6.9. A very detailed study of kinks made by Smalyukh and Lavrentovich can be found in the reference [27].

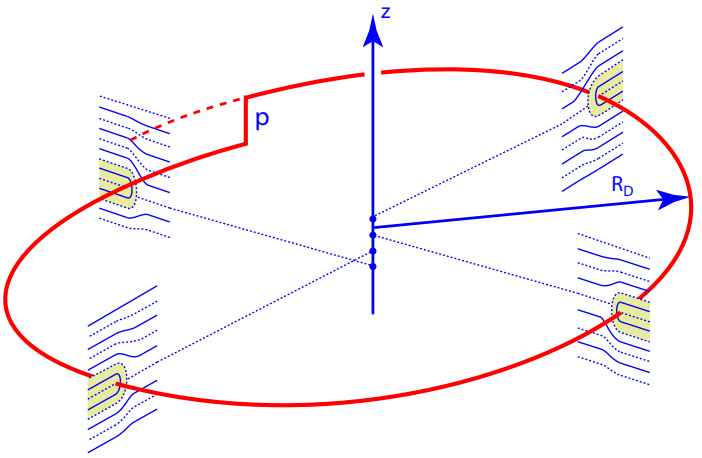

Figure 7. Helical shape of a dislocation loop in its ground state. Here it is buckled with one kink of height p.

4.5. *Helical shape of dislocation loops*

The tension T of the thick dislocation depends also on its orientation. The expression (5) is valid only for the dislocation parallel to the y axis. For different azimuthal directions of the dislocation making the angle ψ is with the y axis, the expression (5) has to be modified as follows

$$T(z_D,\psi) = T_0 + \Delta T \sin^2\left(2\pi z_D/p - \psi\right) \tag{6}$$

As required, this new expression is invariant with respect to the symmetry operations of the cholesteric mesophase that associate rotation by the angle ψ with the translation $\Delta z = p\psi/(2\pi)$. For example, the minimum of the tension given by equation (6)

$$T(z_D, psi) = T_0 \tag{7}$$

occurs for

$$z_D = p\frac{\psi}{2\pi} \tag{8}$$

This condition is satisfied in particular when the dislocation takes the helicoidal shape given by

$$\begin{aligned} x_D &= R_D\cos(\psi) \\ y_D &= R_D\sin(\psi) \\ z_D &= p\frac{\psi}{2\pi} \end{aligned} \tag{9}$$

where R_D is the radius of the helix (see Figure 7).

In conclusion, a dislocation loop in its ground state cannot be flat; is must take a helicoidal shape buckled with one kink of height p or with two kinks of height $p/2$.

4.6. *Bridge-like crossings of dislocations*

The relationship $z_D = p\psi/(2\pi)$ between the orientation of a dislocation (expressed by the azimuthal angle ψ and its z position inside the cholesteric helix has another important consequence concerning crossings of dislocations such as the on in Figure 4 (g) discussed previously.

The scheme of the crossings depicted in Figure 4 (g) shows that it is bridge-like because the two dislocations crossing each other have different orientations ψ so that their z position cannot be same.

Let us stress that systems of dislocation lines with the bridge-like crossings remind mathematicians and theorists of knots and links represented by their shadow-like projections on a plane. (In the case of Figure 4 (a), all visible crossings belong to one multiply folded unknot.) They would ask: "do these crossings belong to unknots or to knots or links?".

5. Discovery of the Hopf link made of dislocations

This issue was initiated by Bouligand in one of his papers on textures and defects in cholesterics [22], beautifully illustrated with pictures taken with a microscope and with his own handmade drawings. In his paper, Bouligand reports on the presence of pairs of interlaced dislocation loops such the one shown in Figure 8 (a).

The discovery of this texture, called by Bouligand "double anneau", inspired indeed theorists and lead to publication in 1978 of the article untitled "Distortions with double topological character [20]: the case of cholesterics" that Bouligand cosigned with B. Derrida, V. Poénaru, Y. Pomeau and Gérard Toulouse. As stressed in the title, the "double anneau" configuration has a *double topological character*:

(1) dislocations themselves are linear topological defects of the cholesteric order parameter,
(2) simultaneusly, the interlaced rings have the nontrivial topology of the Hopf link.

Surprisingly, to our knowledge, the observation by Bouligand of the "double anneau" texture was not confirmed for decades in spite of the fact that patterns of dislocations of cholesteric liquid crystals called commonly "oily streaks" were extensively studied and displayed in articles

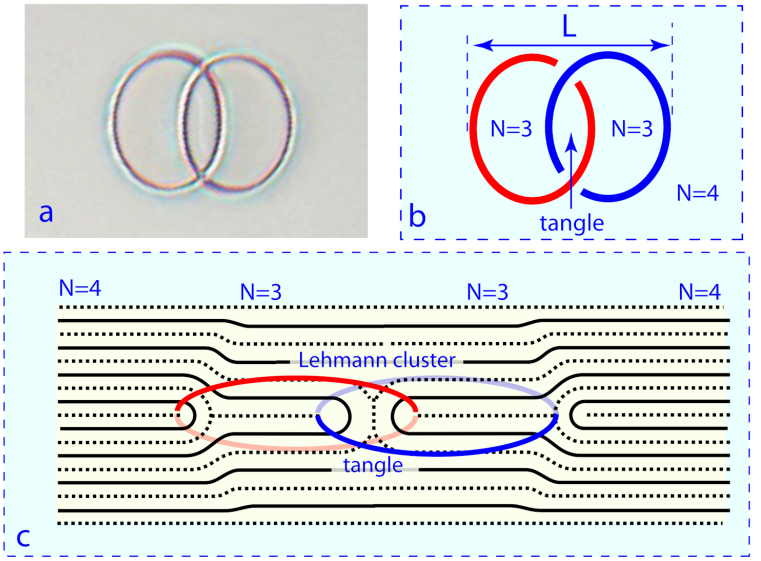

Figure 8. The "double anneau" texture made of dislocations discussed in references [22] and [20]. a) Microscopic picture obtained in a recent experiment with a cholesteric sample (5CB/CB15) confined in the crossed cylinders geometry. b) Geometry of the interlaced dislocation loops observed from above. c) Side view of the cholesteric texture.

and books. As a possible explanation of this anomaly we could invoke the fact that the articles of Bouligand were written in French so that the findings reported by Bouligand remained wrongfully in shadow.

6. Distortions with the double topological character, new experiments

6.1. *Setup*

Here, we will report on experiments performed recently with the setup depicted schematically in Figure 4 (b), which was built with the purpose to illustrate with color pictures of dislocations an article written in honor of Maurice Kleman [24] who passed away in 2021, two years before Gérard Toulouse. In this setup (see Figure 4 (b)), a cholesteric droplet is maintained by capillarity between between two identical crossed cylindrical mica sheets. Using the mica sheets instead of the glass slides has three advantages:

(1) surfaces of freshly cleaved mica sheets are perfectly clean
(2) their atomic crystalline structure is anisotropic and has the suitable property of orienting the molecules of the cholesteric of in one direction parallel to the mica surface
(3) thin mica sheets being very flexible are easy to bend

As the thickness of the cylinder/cylinder gap varies as:

$$h(x,y) \approx h_{min} + \frac{x^2+y^2}{2R_m} = h_{min} + \frac{r^2}{2R_m} \tag{10}$$

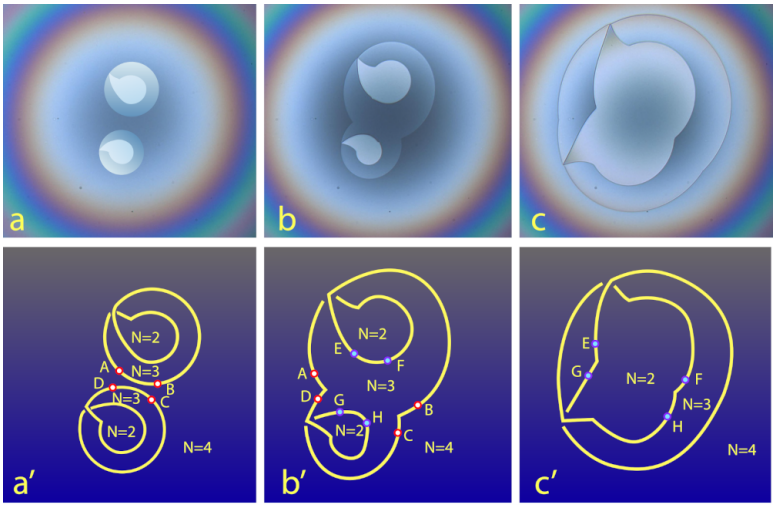

Figure 9. Genesis of the Hopf link. a-a') Nucleation of two folded unknots. b-b') Coalescence of the external loops of the two colliding folded unknots. c-c') Coalescence of the internal loops of the folded unknots. The pictures a-c are snapshots taken during the experiment. (see videos 4 and 5)

where R_m is the radius of curvature of the mica sheets, dislocations are expected to form in equilibrium a target-like pattern made of concentric circles with radii r_N satisfying the equation

$$p(N+1/2) = h_{min} + \frac{r_N^2}{2R_m} \tag{11}$$

where N is an integer.

6.2. *Nucleation of folded unknots*

With the aim to test this prediction we made a detailed study of nucleation of dislocation loops driven by a compressive strain of cholesteric layers squeezed between the cylindrical mica sheets. We expected that a slow compression of the gap (reduction of the minimal thickness h_{min}) should result in nucleation, one after another, of circular individual concentric dislocation loops with decreasing index N forming together a target-like pattern.

Surprisingly, when the initial thickness h_{min} of the gap expressed in units of p, $N = h_{min}/p$, was for example of the order of 10, several dislocation loops were nucleated in one burst and they were not individual but interconnected by crossings into folded "superloops". An example of such a superloop is shown in Figure 4 (d)) where five loops labeled from 1 to 5 are interconnected by crossings such as the one between the loops 1 and 2 represented in the insert 4 (g).

For the sake of simplicity, let us consider the second example of the folded superloops shown in Figure 9 (a) and (a'). Here, two superloops were nucleated simultaneously. They are made of two loops connected by one crossing. From topological point of view they are folded (twisted) unknots. Theoretically, the crossing could be removed by the Reidemeister move "untwist" so that the folded unknots would be transformed into a trivial circular unknots. However, in practice, the "untwist" move is energetically forbidden in the crossed cylinders geometry so that the folded unknot configuration is stable as long as the minimal thickness remains small enough.

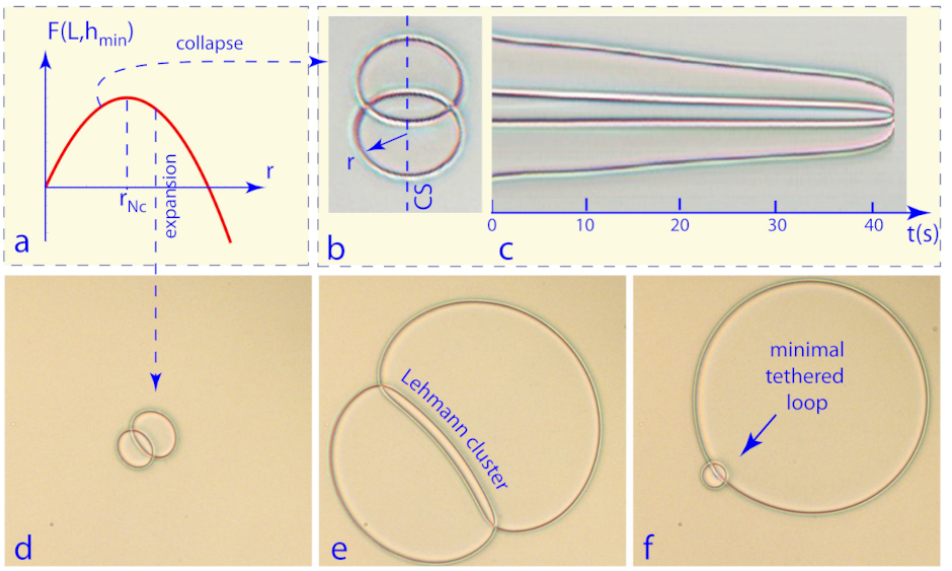

Figure 10. Instability of the Hopf link. a) Variation of the energy of dislocation loops with their radius r. b) Symmetrical configuration of the Hopf link. In this picture, its size is smaller than the critical one r_{Nc} given by equation (12). c) Spatio-temporal cross section showing the shrinking and the final the collapse of the Hopf link. d) Almost symmetrical configuration of the Hopf link. e) When $r > r_{Nc}$ the interlaced loops expand until they reach their equilibrium size. They remain associated by the dislocations' pair known as the Lehmann cluster. f) On a longer time scale, the length of the Lehmann cluster is reduced for energetical reasons so that the smaller dislocation loop shrinks until it reaches its minimal size. One obtains an asymmetric configuration, called *necklace*, of the minimal loop tethered on the large loop. (see videos 6, 7 and 8)

6.3. *Coalescence of two folded unknots into the Hopf link*

The second surprise came when, during their expansion, the two folded unknots collided (see Figures 9 (a) and (a')). First, the external dislocations loops of the two unknots coalesced (merged) (see Figures 9 (b) and (b')). The coalescence can be seen as a rewiring process resulting from the collision of the AB and CD segments: $AB + CD \Rightarrow AD + BC$. As a result, the two folded unknots became connected into one unknot folded twice.

Finally, the expansion of the two internal folds lead to a new collision followed by the coalescence of the folds: $EF + GH \Rightarrow EG + FH$. The result of the two successive collision-coalescence events is shown in Figures 9 (c) and (c'): the crossings of the two unknots are gathered together into the elementary Hopf link.

Let us stress that this method of producing the Hopf link is reproducible because nucleation of the folded unknots is heterogenous and occurs always at the same points – locations of the nucleation centres.

6.4. *Instability of the symmetrical configuration of the Hopf link*

After the first identification of the Bouligand's "double anneau" made of interlaced dislocation loops in our samples with large pitches ($p \approx 40\mu m$) (see Figure 8 (a)), we reexamined videos

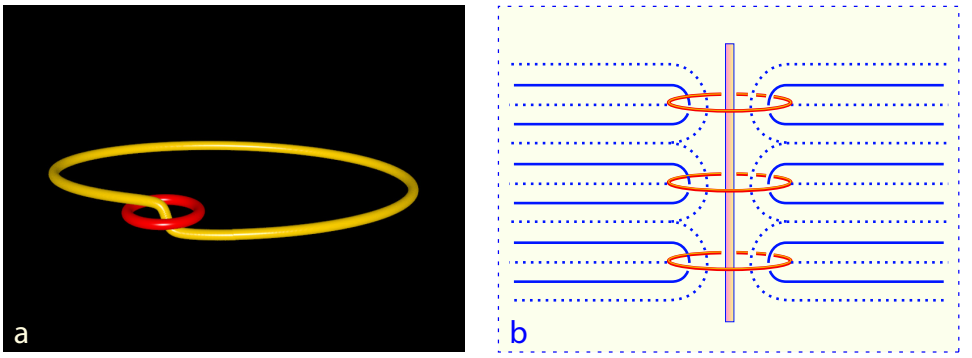

Figure 11. Necklace configurations of the Hopf link. a) One minimal loop tethered on the kink of the large cargo loop. b) Periodic system of minimal loops tethered on a straight screw dislocation imagined by Rault [28].

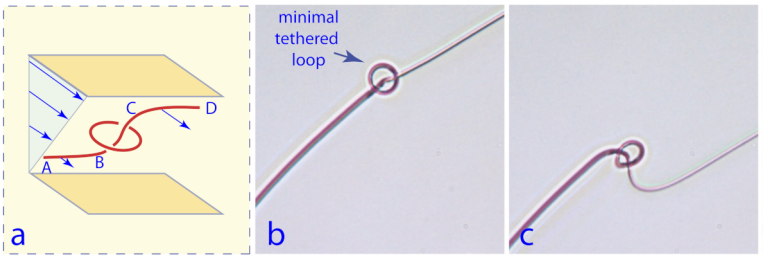

Figure 12. Robustness of the Hopf link in its necklace configuration with respect to a shear deformation. a) Geometry of the experiment. b-c) Deformation of the necklace unveils its three dimensional structure.

recorded in previous experiments and have found that in fact the Hopf links were occurring quite frequently in them. The reason for which we did not identified them previously is the following.

The Hopf link is usually represented as two interlaced loops of the same size (see Figure 8 (b)) even if from topological point of view the size of the interlaced loops does not matter. In practice, such a symmetrical configuration is energetically unstable and evolves in two different ways. Let us suppose that (1) the Hopf link is located in the center of the crossed cylinders gap where the thickness h(x,y) is minimal and (2) the sizes of the interlaced rings are the same $r \approx L/2$. It can be shown that due to the tension T of dislocations (energy par unit length), there exist the critical radius r_{Nc} (see Figure 8 (a))

$$r_{Nc} = p\frac{\widetilde{T}}{h_N/h_{min}-1} \tag{12}$$

with $\widetilde{T} = T/(4\pi K_{22})$ and $h_N = p(N+1/2)$, defining two different cases:

(1) for $r < r_{Nc}$, the interlaced loops will shrink and the Hopf link will collapse as it is shown in Figures 10 (b) and (c),

(2) for $r > r_{Nc}$ (Figure 10 (d)), the interlaced loops will expand into the configuration shown in Figure 10 (e) in which they remain associated by the dislocations' pair known as the Lehmann cluster. The Lehmann cluster has some energy per unit length so that on a longer time scale it shrinks until the smaller dislocation loop reaches its minimal size

(see Figure 10 (f)). The asymmetric configuration of the *minimal loop tethered on the larger cargo loop* will be called below *necklace*.

In conclusion, the symmetrical configuration of the Hopf link is unstable and therefore exceptional. The asymmetric necklace configuration is therefore the most frequent. However, as the diameter of the minimal loop is of the order of p, in samples with very short pitches $p < 10\mu m$, the minimal tethered loops are hardly visible at low magnifications and can be easily confused with impurities trapped by the larger cargo loop. For example in Figure 14 (h) discussed in Section 6.8, 17 minimal loops are threaded on the cargo loop but they are invisible on this picture taken at low magnification. In the Figure 14 (h) obtained with a seven times larger magnification, the dislocation became visible.

6.5. *Robustness of the Hopf link, in its necklace configuration, with respect to a shear deformation*

In ref. [20], the Hopf link made of the dislocations with the Burgers vector $b = p$ (called "J" in ref. [20]) has been termed "topological atom" because the interlaced dislocation loops cannot be easily unlinked without a local destruction of the cholesteric order. This kind of the robustness of the Hopf link appears in the experiment depicted in Figures 12 where a shear flow driven by the horizontal motion of the upper mica sheet is applied to the sample. Viscous forces acting on the minimal and large loops, deforms them strongly. In spite of that, no matter how large is this deformation, the minimal loop remains tethered on the large one.

By the way, let us stress that this experiment unveils the geometry of the cargo loop in the vicinity of the minimal loop. Let $z = 0$ be the level of the minimal loop. The cargo loop is made of two segments AB and CD located at different levels, $z_{AB} = -p/2$ and $z_{CD} = p/2$, and connected by a kink of height $z_{AB} - z_{CD} = p$. In first approximation, the kink can be seen as a vertical segment BC of the cargo loop passing through the center of the minimal loop.

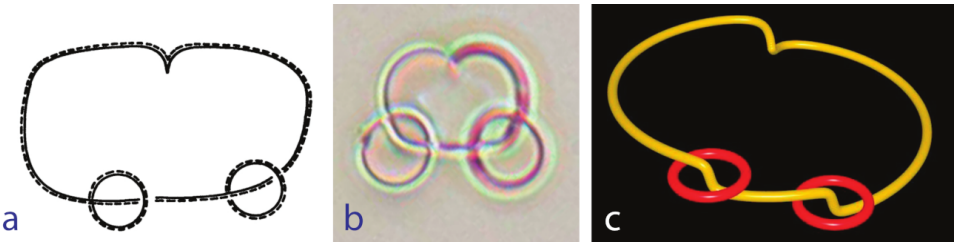

Figure 13. "The triple ring structure" predicted in ref. [20]. a) Reproduction of [20, Figure 1]. b) The three components Hopf link observed in our experiments. c) Perspective view showing three kinks on the cargo loop carrying the two minimal loops. (see videos 9, 10 and 11)

6.6. *Necklace configuration of the Hopf link*

The large cargo loop of the necklace configuration has, as expected, the helical shape and is buckled with the kink of height p (see Figure 11 (a)). The minimal loop, tethered on this kink of cargo loop, is flat (see Figure 11 (a)) because the kink can be seen as a short segment of a nonsingular vertical screw dislocation with the Burgers vector $b = p$. This configuration of flat edge dislocation loops tethered on a vertical screw dislocation has been imagined and discussed for the first time by Rault [7, 28].

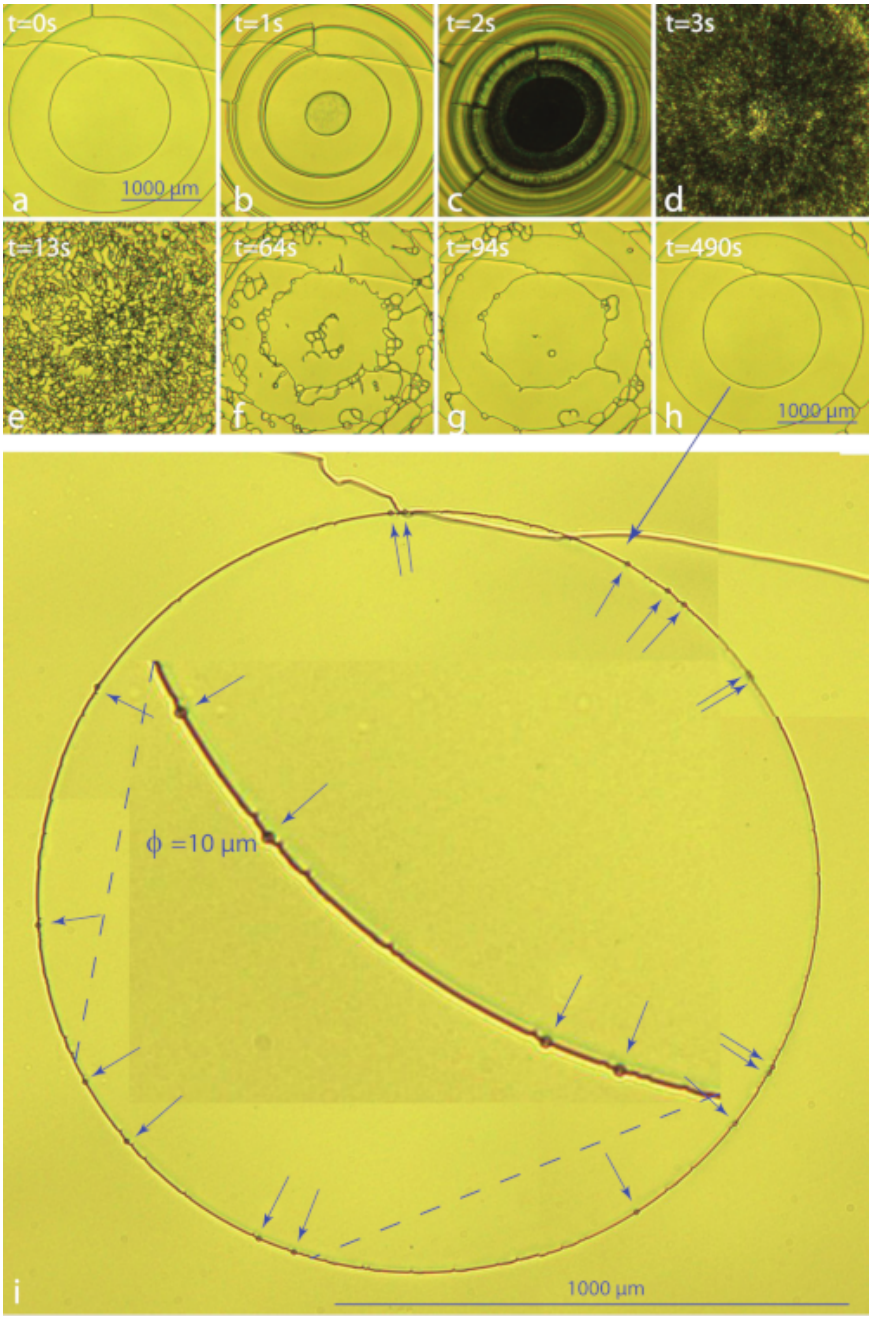

Figure 14. Topological transition: transformation of a trivial unknot into a multiple Hopf necklace by a strong perturbation of the minimal gap thickness h_{min}. a) Circular dislocation loop in the centre of the cylinder/cylinder gap. It has the topology of a trivial unknot. b-d) Perturbation of the cholesteric texture induced by a rapid increase of the minimal gap thickness. d-h) Relaxation after the recovery of the initial gap thickness. h) The dislocation loop in the centre carries now 17 minimal loops visible at a higher magnification in the picture i. i) The multiple Hopf necklace. The 17 minimal loops are indicated by arrows. Their diameter is of the order of the cholesteric pitch $p_o \approx 10\mu m$.

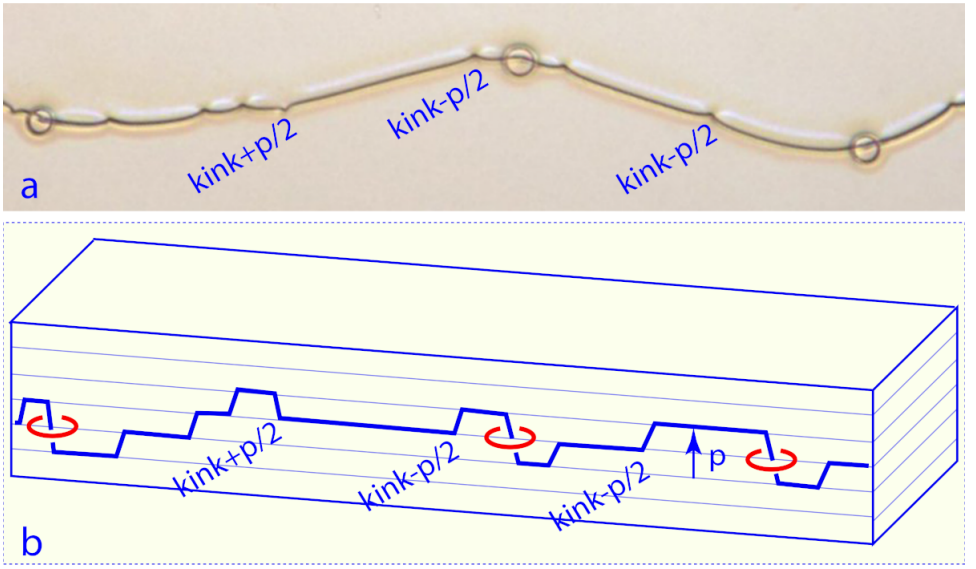

Figure 15. Segment of a Hopf necklace with three minimal loops tethered on a cargo dislocation containing several $\pm p$ kinks. a) Vue in a microscope. b) Perspective view.

6.7. *Necklace configuration of the double Hopf link*

After the first identification of the Hopf link in its necklace configuration we have found that several minimal loops can be tethered on one cargo loop. In particular, we observed (see Figure 13 (b) the configuration of two minimal loops tethered on the cargo loop represented in Figure 13 (a) which was conjectured in the article of Bouligand at al. [20]. The perspective view in Figure 13 (c) allows to identify three kinks on the cargo loop. The two minimal loops are tethered on kinks of height $\Delta z_1 = \Delta z_2 = -p$. The third kink, called cuspoidal in ref. [20] has opposite sign: $\Delta z_c = +p$.

The total change of the height z due to these three kinks encountered on a anticlockwise circuit along the cargo loop is thus $\Delta z_1 + \Delta z_2 + \Delta z_c = -p$. Let us remind that, as discussed in Section 4.5, the change of the azimuthal direction of the cargo loop by $\Delta\psi = 2\pi$ results in the change of height of $\Delta z_{loop} = +p$.

After taking into account all contributions we have

$$\Delta z_1 + \Delta z_2 + \Delta z_c + \Delta z_{loop} = 0 \tag{13}$$

This conservation law written in a different form was used by Bouligand et al. [20] for prediction of the "tripple ring" configuration.

6.8. *Generation of multiple Hopf necklaces*

During submission of this paper we have found that the multiple Hopf necklaces can be generated in a system of the coaxial dislocation loops (folded or not) by strong step-like perturbations of the minimal gap thickness:

$$h_{min} \approx 3p_o \Rightarrow_{1s} 30p_o \Rightarrow_{2s} \Rightarrow 3p_o \tag{14}$$

Figure 14 shows a typical example of such a process. The initial texture of dislocation loops in Figure 14 (a) is made of a trivial unknot in the centre surrounded by folded unknots. The series of

next three pictures shows that the perturbation expressed in equation (14) generates a very dense system of dislocations (not well identified so far) which relaxes elastically to the texture shown in Figure 14 (h) which seems to be identical to the initial one in Figure 14 (a).

This appearance is misleading because at a higher magnification a system of 17 minimal loops tethered on the large cargo loop can be identified. They were invisible in the Figure 14 (h) because their diameter $\phi \approx po = 10\mu m$ is very small.

Obviously, when cholesteric samples with much smaller pitches $p_o < 1\mu m$ are used, the minimal loops can be hardly resolved optically.

This is probably the reason for which beside the papers of Bouligand [22] and Bouligand et al. [20] the Hopf necklaces have not been mentioned elsewhere.

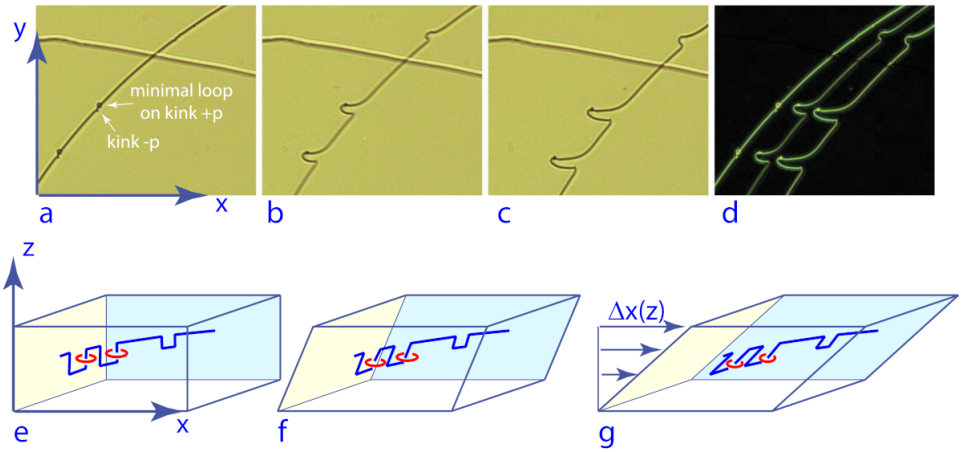

Figure 16. Behaviour of a Hopf necklace with two minimal loops in a shear flow. a-d) Views in a microscope. e-g) Perspective view.

6.9. *Stability of the Hopf necklaces*

The third example of the Hopf necklaces shown in Figure 15 was obtained using a sample with a much larger pitch $p_o \approx 100\mu m$. We can identify here three minimal loops tethered on the $\Delta z_k = -p$ kinks of the cargo loop. Beside them, there are several cuspoidal points corresponding to $\pm p/2$ kinks. The cuspoidal kinks can move along the cargo loop and assemble into kinks of height $\Delta z_c = p$. Such free kinks of height $\Delta z_c = p$ are enemies of the minimal loops: the minimal loops can be incorporated into the cargo loop after their encounters with the kinks.

In spite this threat, necklaces are quite resilient and can stand, for example, strong deformations imposed by a shear flow. As an example we show in Figures 16 (a), (b) and (c) the deformation, in a shear flow, of a necklace segment with two minimal loops threaded on the cargo loop. To be more precise, we should rather say that the minimal loops are threaded on +p kinks. Let us also stress that these +p kinks are accompanied by -p kinks. The cargo loop has thus a crenellated shape which is unveiled by the shear flow as depicted in Figures 16 (e), (f) and (g).

We postpone a more detailed discussion of this issue to another paper.

7. Conclusions

« Long temps me fut nécessaire pour comprendre les tenants et les aboutissants de ma vocation, singulière ».

The sound of this sentence, written by Gérard Toulouse at the beginning of a short text untitled "Le sens d'une exploration" and published in the book "Le goût de la science" [29], unveils the subtle and engaging soul of Gérard.

As already said in the Introduction, one of the authors of the present article (P.P.), as a PhD student, had the chance to listen to his wonderful lectures on topological aspects of physics in the Laboratoire de Physique des Solides in Orsay. Many years later, as a lecturer at Ecole Normale rue Lhomond, he met Gérard again who, at the end of this encounter, generously offered him the book mentionned above.

Today, another classical text comes on mind: *"Exegi monumentum aere perennius... Non omnis moriar..."*. The legacy of Gérard contains written contributions which like those of Horace, were, are and will be quoted. However, among the traces left by Gérard even more important are those that are *invisible to the eye:* his impacts on minds. The present article reporting on recent experiments with topological defects and with knots and links is like a plant grown from a seed sown by Gérard many years ago.

Acknowledgements

We thank Yves Pomeau and Bernard Derrida for the invitation to participate to the memorial issue of Comptes Rendus de l'Académie des Sciences in honor of Gerard Toulouse. The redaction of our contribution stimulated greatly the recent experiments on the "objects with the double topological character" i.e. on the links and necklaces made of dislocation loops in cholesterics.

We address our thanks for the hospitality to Yvan Smalyukh at the "International Institute for Sustainability with Knotted Chiral Metamatter (WPI-SKCM2)".

The experimental setup tailored for production of the cholesteric dislocations in the cylinder/cylinder mica wedges was inspired by discussions with M. Zeghal and built by V. Klein, J. Sanchez and S. Saranga. We also benefitted from discussions with Y. Pomeau, P. Oswald, Y. Smalyukh, O. Lavrentovich, A. Leforestier and C. Goldmann as well from the help of I. Settouraman, Y. Simon, M. Bottineau, J. Vieira and I. Nimaga.

We would like also to thank the referee for constructive remarks and queries.

Declaration of interests

The authors do not work for, advise, own shares in, or receive funds from any organization that could benefit from this article, and have declared no affiliations other than their research organizations.

References

[1] G. Toulouse and M. Kleman, "Principles of a classification of defects in ordered media", *J. Physique Lett.* **37** (1976), pp. 149–151.

[2] J. Friedel, *Dislocations*, International series of monographs on solid state physics, Pergamon Press, Oxford, 1964.

[3] P. Pieranski, "Dislocations and other topological oddities", *C. R. Acad. Sci. Paris* **17** (2016), pp. 242–263.

[4] P.-G. de Gennes, *Superconducivity of metals and alloys*, Benjamin, 1964.

[5] P. Pieranski, "Pierre Gilles de Gennes: beautiful and mysterious liquid crystals", *C. R. Acad. Sci. Paris* **20** (2019), pp. 756–769.

[6] M. Kleman and O. Lavrentovich, *Soft matter physics: an introduction*, Partially Ordered Systems, Springer, 2003.

[7] M. Kurik and O. Lavrentovich, "Defects in liquid crystals: homotopy and experimental studies", *Usp. Fiz. Nauk* **154** (1988), pp. 381–431.

[8] I. Smalyukh, "Review: knots and other new topological effects in liquid crystals and colloids", *Rep. Prog. Phys.* **83** (2020), article no. 106601.

[9] M. W. Scheeler, D. Kleckner, D. Proment, G. L. Kindlmann and W. T. M. Irvine, "Helicity conservation by flow accross scales in reconnecting vortex links and knots", *Proc. Natl. Acad. Sci. USA* **111** (2014), pp. 15350–15355.
[10] L. Embon, Y. Anahory, Z. L. Jelić, et al., "Imaging of super-fast dynamics and flow instabilities of superconducting vortices", *Nat. Commun.* **8** (2017), article no. 85.
[11] M. V. Berry and M. R. Dennis, "Knotted and linked phase singularities in monochromatic waves", *Proc. R. Soc. Lond., Ser. A* **111** (2001), pp. 2251–2263.
[12] P. Manneville, *Dissipative structures and weak turbulence*, Perspectives in Physics, Academic Press Inc., Boston, 1990.
[13] T. Passot and A. C. Newell, "Towards a universal theory for natural patterns", *Phys. D: Nonlinear Phenom.* **74** (1994), pp. 301–352.
[14] P. Pieranski, E. Dubois-Violette and E. Guyon, "Heat convection in liquid crystals heated from above", *Phys. Rev. Lett.* **30** (1973), pp. 736–739.
[15] P. Pieranski and E. Guyon, "Effects of elliptically polarized shear flows in nematics", *Phys. Rev. Lett.* **39** (1977), pp. 1280–1282.
[16] S. Douady and S. Fauve, "Pattern selection in Faraday instability", *Eur. Phys. Lett.* **6** (1988), article no. 221.
[17] J.-M. di Meglio, D. A. Weitz and P. M. Chaikin, "Competition between shear melting and Taylor instabilities in colloidal crystals", *Phys. Rev. Lett.* **58** (1987), pp. 136–139.
[18] J. Hulin, P. Pieranski, M. Fermigier, et al., "Hommage à Etienne Guyon", *Reflets phys.* **Mai** (2024), no. 78, pp. 32–41.
[19] M. Dazza, L. Cabeca, S. Copar, M. H. Godinho and P. Pieranski, "Action of fields on captive disclination loops", *Eur. Phys. J. E* **40** (2017), article no. 28.
[20] Y. Bouligand, B. Derrida, V. Poénaru, Y. Pomeau and G. Toulouse, "Distorsions with double topological character: the case of cholesterics", *J. Phys. France* **39** (1978), pp. 863–867.
[21] P. Pieranski and M. H. Godinho, "Unknots, knots, links and necklaces made of dislocations in cholesterics", *Liquid Crystals* (2024).
[22] Y. Bouligand, "Recherches sur les textures des états mésomorphes. 6 - Dislocations coin et signification des cloisons de Grandjean–Cano dans les cholestériques", *J. Phys.* **35** (1974), pp. 959–981.
[23] P. Pieranski and M. H. Godinho, "Fertile metastability", *Liquid Crystals* (2023), pp. 1–16.
[24] P. Pieranski, "Cholesteric dislocations in mica wedges", *Liquid Crystals Reviews* **10** (2022), pp. 6–33.
[25] G. Friedel, "Etats mésomorphes de la matière", *Ann. Phys. Fr.* **18** (1922), pp. 273–474.
[26] M. Kleman and J. Friedel, "Lignes de dislocations dans les cholestériques", *J. Phys. Colloques* **30** (1969), pp. C4-43–C4-53.
[27] I. I. Smalyukh and O. D. Lavrentovich, "Three-dimensional director structures of defects in Grandjean–Cano wedges of cholesteric liquid crystals studied by fluorescence confocal polarizing microscopy", *Phys. Rev. E* **6** (2002), article no. 051703.
[28] J. Rault, "Dislocation χ dans les cholestériques: II. Modèles des dislocations χ", *Philos. Mag.* **29** (1974), pp. 621–640.
[29] G. Toulouse, "Sens d'une exploration", in *Le goût de la science. Comment je suis devenu chercheur* (J. Clarini, ed.), Editions Alvik, 2005.